

Transference of Love-type waves in a bedded structure containing a functionally graded material and a porous piezoelectric medium*

S. MONDAL, S. A. SAHU[†], K. K. PANKAJ

Department of Applied Mathematics, Indian Institute of Technology (ISM),
Dhanbad 826004, Jharkhand, India

(Received Oct. 30, 2018 / Revised Feb. 21, 2019)

Abstract The frequency of the Love-type surface waves in a bedded structure consisting of a porous piezoelectric (PP) medium and a functionally graded material (FGM) substrate is approximated. The FGM layer is assumed to have a constant initial stress. The Wentzel-Kramers-Brillouin (WKB) approximation technique is used for the wave solution in the FGM layer, and the method of separation of variables is applied for the solution in the porous piezoelectric medium. The dependence of the wave frequency on the wave number is obtained for both electrically open and short cases. The effects of the gradient coefficient of the FGM layer, the initial stresses (tensile stress and compressive stress), and the width of the FGM layer are marked distinctly and shown graphically. The findings may contribute towards the design and optimization of acoustic wave devices.

Key words porous piezoelectric (PP) material, functionally graded material (FGM), Love-type wave, Wentzel-Kramers-Brillouin (WKB) approximation

Chinese Library Classification O347.4

2010 Mathematics Subject Classification 74B10, 74J15, 74J30

Nomenclature

c_{ijkl} ,	elastic constant of the functionally graded material (FGM) layer;	$\sigma'_{ij} (\sigma^*)$,	stress component in the porous piezoelectric (PP) medium for the solid (fluid) phase;
ε_{ij} ,	dielectric constant of the FGM layer;	$s'_{ij} (s^*)$,	strain component in the PP medium for the solid (fluid) phase;
ρ^f ,	mass density of the FGM layer;	σ^0_{kj} ,	initial stress tensor;
D_i ,	electric displacement vector in the FGM layer;	c'_{ijkl} ,	elastic constant of the PP medium;
α ,	gradient factor of the FGM layer;		

* Citation: MONDAL, S., SAHU, S. A., and PANKAJ, K. K. Transference of Love-type waves in a bedded structure containing a functionally graded material and a porous piezoelectric medium. *Applied Mathematics and Mechanics (English Edition)*, 40(8), 1083–1096 (2019) <https://doi.org/10.1007/s10483-019-2505-6>

[†] Corresponding author, E-mail: ism.sanjeev@gmail.com

©Shanghai University and Springer-Verlag GmbH Germany, part of Springer Nature 2019

$D'_i (D_i^*),$	electric displacement vector in the PP medium for the solid (fluid) phase;	$e'_{ijkl}, e_i^*, \varsigma_{ijk}, \varsigma_i,$	medium; piezoelectric constants of the PP medium;
$E'_i (E_i^*),$	electric field vector in the PP medium for the solid (fluid) phase;	$\varepsilon'_{ij}, \varepsilon_{ij}^*, A_{ij},$	dielectric constants of the PP medium;
$m_{ij},$	elastic constant of the PP medium;	$\varphi^p (\varphi^*),$	electric potential function in the PP medium for the solid (fluid) phase.
$R,$	elastic constant of the PP		

1 Introduction

Piezoelectric materials are smart materials capable of producing electrical fields under mechanical stress. When such materials are embedded in composite structures, smart structures will form. Piezoelectric materials have extensive applications, e.g., actuators, sensors, surface acoustic wave (SAW) devices, and transducers^[1–2]. Despite numerous applications, the smart structures consisting of piezoelectric materials have many shortcomings. Piezoelectric materials are brittle, which may cause failure of piezoelectric material devices under electrical and mechanical loading. Piezoelectric materials cannot be utilized in undersea applications since they have high acoustic impedance. These limitations can be overcome by introducing porosity in a controlled manner to the piezoelectric material (hence reducing the material density). The piezoelectric materials containing tailored porosity are called porous piezoelectric materials. They show specific attributes that cannot be exhibited by their regular dense analogues. Such materials have tremendous utilization in ultrasonic transducers, hydrophones, etc.

Functionally graded materials (FGMs) are a class of materials made of more than one constituent phases. In FGMs, the mechanical properties, i.e., Poisson's ratio, Young's modulus, shear modulus of elasticity, and density, vary continuously and smoothly in the preferred direction^[3]. FGMs have wide applications in solar cells, spacecraft heat shields, biomedical implants, thermoelectric generators, heat exchange tubers, sensors, etc. They can also be used in the medical field for dentistry, skins, and artificial bones^[4].

Since the material properties of the FGM layer is non-uniform and the thermal expansion, chemical shrinkage, etc. are prominent, the presence of initial stresses is unavoidable in an FGM layered structure. Moreover, the layered structure is pre-stressed to prevent from brittle fracture. The initial stresses in the layered structures can lead to delamination, microcracking, debonding, and degradation of the layer. Therefore, the effects of the initial stresses on the existence and propagation behavior of transverse surface waves in such layered structures are important to be investigated.

The compositions of FGMs and porous piezoelectric ceramics can reduce the brittleness of the composite structures, which leads to the enhancement of the strength and results in the increase in the performance of the devices. In recent years, the study of shear wave propagation in FGM composite structures has turned into a focus point of many researchers. Han et al.^[5] studied the transmission of elastic waves in FGM plates with a numerical method. They divided the FGM layer into quadratic layer elements (QELs), and presented a characterization of the material property of the FGM. Han and Liu^[6] used a computational technique to analyze the propagation of shear waves in FGM plates. Qian et al.^[7] obtained the analytical solutions for the transference of Love-type waves in a structure consisting of an FGM layer lying over the piezoelectric half-space with the Wentzel-Kramers-Brillouin (WKB) asymptotic technique. Zhang and Batra^[8] studied the transmission of elastic waves in FGMs with a modified smoothed particle hydrodynamics method. Bin et al.^[9] used the Legendre orthogonal polynomial series expansion approach to explore the propagation of harmonic waves in functionally graded magneto-electro-elastic plates. Qian et al.^[10] used the WKB technique to study the Love-type wave propagation in the FGM half-space. Aksoy and Şnocak^[11] adopted the space-

time discontinuous Galerkin method to examine the wave propagation in layered materials. Ravasoo^[12] studied the counter-propagation of two ultrasonic harmonic waves in an inhomogeneous material having exponentially varying physical properties. Cao et al.^[13] analyzed the effects of the gradient coefficient on the Lamb wave propagation in an FGM plate with the power series method. Kielczyński et al.^[14] investigated ultrasonic Love-type waves in the FGMs having inhomogeneity. Arani et al.^[15] studied the effects of the material in-homogeneity on the electro-thermo-mechanical behaviors of a rotating hollow circular shaft made from functionally graded piezoelectric material (FGPM). Sahu et al.^[16] studied the shear wave propagation in a composite structure consisting of an FGPM layer bonded between a piezomagnetic layer and the elastic half-space. Singhal et al.^[17] investigated the transmission of the surface waves in an FGPM layer sandwiched between a piezomagnetic (PM) layer and a piezoelectric (PE) substrate having initial stress. Mondal and Sahu^[18] studied the propagation of shear horizontal (SH) waves in a corrugated FGPM layer lying over a piezomagnetic half-space.

Remarkable works have been performed addressing the propagation of waves in composites consisting of porous piezoelectric materials. Craciun et al.^[19] investigated the propagation of elastic waves in porous piezoelectric ceramics. The influence of porosity on the properties of porous piezoelectric materials has been experimentally studied by many authors^[20–22]. Kar-Gupta and Venkatesh^[23] used the finite element method to study the effects of porosity on piezoelectric materials. Vashishth and Gupta^[24] derived the constitutive and dynamical equations for porous piezoelectric materials. Vashishth et al.^[25] investigated the propagation of a Bleustein-Gulyaev (B-G) type wave in a layered porous piezoceramic structure. Gaur and Rana^[26] analytically studied the SH wave propagation in a two-layered composite structure comprising porous piezoelectric and piezoelectric materials. Vashishth and Gupta^[27] studied the dispersion of waves in a porous piezoelectric (PP) medium with the Christoffel equation. Baroi et al.^[28] studied the propagation of SH waves in a viscous liquid overlying a porous piezoelectric half-space. Despite these works, the wave propagation in a PP layer still needs more investigation. There are certain characteristics of PP materials revealed to get contrast findings in wave propagation phenomena.

In this paper, the propagation behaviors of Love-type waves in a structure consisting of an FGM layer and a porous piezoelectric substrate are studied. The FGM layer is assumed to have constant initial stresses. For the solution of the FGM layer, the WKB approximation method is used. For the solution of a porous piezoelectric medium, the variable separable method is used. Both electrically open and short cases are considered. The dispersion relation is obtained in the determinant form for each case. Numerical examples are given to exhibit the analytical results graphically. The effects of the material gradient of the FGM layer and the initial stresses (tensile and compressive stresses) on the velocity profile of the Love-type wave are shown clearly. The dependence of height of the FGM layer on the velocity of the considered wave is illustrated. The obtained results can be utilized for the improvement of piezoelectric devices.

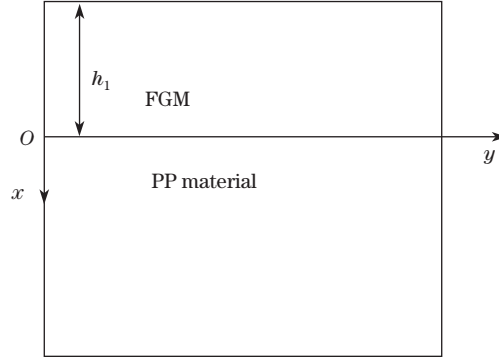
2 Formulation of the problem

We contemplate the Love-type wave propagation in a bedded structure comprising of an FGM layer and a porous piezoelectric substrate (see Fig. 1). In the Cartesian coordinate system, the x -axis lies vertically down and the y -axis extends in the wave propagation direction. We assume that the FGM layer has constant initial stresses and the surface is traction-free. Usually, for SAW devices, the thickness of the substrate is much larger than that of the layer. Therefore, the structure may be treated as a layer-half-space problem.

2.1 Formulation for the FGM layer

For the wave motion with small amplitude, the field equations can be expressed as follows^[10]:

$$\sigma_{ij,j} + (u_{i,k}\sigma_{kj}^0)_j = \rho\ddot{u}_i, \quad D_{i,i} = 0, \quad (1)$$

**Fig. 1** Geometry of the problem

and the constitutive relations are as follows:

$$\sigma_{ij} = c_{ijkl} s_{kl}, \quad D_i = \varepsilon_{ij} E_j, \quad (2)$$

where $i, j, k = 1, 2, 3$, and c_{ijkl} and ε_{ij} are elastic and dielectric constants, respectively. ρ is the mass density. u_i denotes the mechanical displacement in the i th-direction. D_i denotes the electric displacement vector. σ_{ij} and σ_{kj}^0 denote the stress tensor and the initial stress tensor, respectively.

The strain tensor is related to the displacement by $s_{ij} = (u_{i,j} + u_{j,i})/2$, and the electric field is related to the electric potential by

$$E_i = -\frac{\partial \varphi}{\partial x_i}, \quad i = 1, 2, 3. \quad (3)$$

Considering the wave propagation in the y -axis, the mechanical displacement components and the scalar electric potential function become

$$u_1 = 0, \quad u_2 = 0, \quad u_3 = w^f(x, y, t), \quad \varphi = \varphi^f(x, y, t). \quad (4)$$

Substituting Eq. (4) into Eq. (1) yields

$$\frac{\partial \sigma_{zx}}{\partial x} + \frac{\partial \sigma_{yz}}{\partial y} + \sigma_y^0 \frac{\partial^2 w^f}{\partial y^2} = \rho \frac{\partial^2 w^f}{\partial t^2}, \quad (5)$$

$$s_x = 0, \quad s_y = 0, \quad s_z = 0, \quad s_{xy} = 0, \quad s_{yz} = \frac{\partial w^f}{\partial y}, \quad s_{zx} = \frac{\partial w^f}{\partial x}, \quad (6)$$

where w^f , ρ^f , c_{44}^f , and φ^f denote the mechanical displacement, the mass density, the shear modulus, and the electric potential in the FGM layer. The mass density is assumed to be constant, while the shear modulus of the FGM layer is considered to be varying exponentially in the thickness direction.

$$c_{44}^f(x) = c_{44}^0 g(x).$$

We assume that $g(x) = e^{\alpha x}$, $c_{44}^0 = c_{44}(0)$, and ρ^f is constant, where α is the gradient coefficient.

Substituting Eqs. (2), (3), (4) into Eq. (1), from Eqs. (5) and (6), we have

$$g' \frac{\partial w^f}{\partial x} + g \frac{\partial^2 w^f}{\partial x^2} + \left(\frac{\sigma_y^0}{c_{44}^0} + g \right) \frac{\partial^2 w^f}{\partial y^2} = \frac{1}{\beta_1^2} \frac{\partial^2 w^f}{\partial t^2}, \quad (7a)$$

$$\frac{\partial^2 \varphi^f}{\partial x^2} + \frac{\partial^2 \varphi^f}{\partial y^2} = 0. \quad (7b)$$

Also, we have the components of σ_{ij} and D_i as follows:

$$\begin{cases} \sigma_x = \sigma_y = \sigma_z = \sigma_{xy} = 0, \\ \sigma_{yz} = c_{44}^0 g \frac{\partial w^f}{\partial y}, \quad \sigma_{zx} = c_{44}^0 g \frac{\partial w^f}{\partial x}, \\ D_x = -\varepsilon_{11} \frac{\partial \varphi^f}{\partial x}, \\ D_y = -\varepsilon_{11} \frac{\partial \varphi^f}{\partial y}, \end{cases} \quad (8)$$

where $\beta_1 = \sqrt{c_{44}^0/\rho^f}$ represents the shear wave velocity at the $x = 0$ interface.

2.2 Formulation for the PP medium

For the PP medium, the equations of motion are as follows^[25]:

$$\begin{cases} \sigma'_{ij,j} = (\rho_{11})_{ij} \ddot{u}_j + (\rho_{12})_{ij} \ddot{U}_j^*, \\ \sigma^*_{,i} = (\rho_{12})_{ij} \ddot{u}_j + (\rho_{22})_{ij} \ddot{U}_j^*, \\ D'_{i,i} = 0, \\ D^*_{i,i} = 0, \end{cases} \quad (9)$$

where u_i and U_i^* are the mechanical displacement components of M_2 , and $(\rho_{11})_{ij}$, $(\rho_{12})_{ij}$, and $(\rho_{22})_{ij}$ are the dynamical mass coefficients.

The constitutive equations for the PP medium are

$$\begin{cases} \sigma'_{ij} = c'_{ijkl} s'_{kl} + m_{ij} s^* - e_{kij} E'_k - \varsigma_{kij} E_k^*, \\ \sigma^* = m_{ij} s'_{ij} + R s^* - \varsigma_k E'_k - e_k^* E_k^*, \\ D'_i = e'_{ijkl} s'_{kl} + \varsigma_i s^* - \varepsilon'_{il} E'_l + A_{il} E_l^*, \\ D^*_i = \varsigma_{ikl} s'_{kl} + e_i^* s^* + A_{il} E'_l + \varepsilon_{il}^* E_l^*, \end{cases} \quad (10)$$

where σ'_{ij} (σ^*) is the stress tensor component for the solid (fluid) phase. s'_{ij} (s^*) is the strain tensor component for the solid (fluid) phase. D'_i (D^*_i) is the electric displacement for the solid (fluid) phase. E'_i (E_i^*) is the electric field vector for the solid (fluid) phase. c'_{ijkl} , m_{ij} , and R are the elastic constants. e'_{ijkl} , e_i^* , ς_{ijk} , and ς_i are the piezoelectric constants. ε'_{ij} , ε_{ij}^* , and A_{ij} are the dielectric constants. Let φ^P (φ^*) be the electric potential function for the solid (fluid) phase.

Then, we have

$$s'_{ij} = \frac{1}{2} \left(\frac{\partial u_i}{\partial x_j} + \frac{\partial u_j}{\partial x_i} \right), \quad s^* = \frac{\partial U_i^*}{\partial x_i}, \quad E'_i = -\frac{\partial \varphi^P}{\partial x_i}, \quad E_i^* = -\frac{\partial \varphi^*}{\partial x_i}. \quad (11)$$

Assume that the waves propagate in the y -axis. Then, the mechanical displacements and the electric potential functions are

$$\begin{cases} u_1 = 0, \quad u_2 = 0, \quad u_3 = w^P(x, y, t), \quad U_3^* = W^*(x, y, t), \\ \varphi = \varphi^P(x, y, t), \quad \varphi^* = \varphi^*(x, y, t), \end{cases} \quad (12)$$

and Eq. (10) can be rewritten as follows:

$$\left\{ \begin{array}{l} \sigma'_{11} = c'_{11}s'_{11} + c'_{12}s'_{22} + c'_{13}s'_{33} + m_{11}s^* - e'_{31}E'_3, \\ \sigma'_{12} = c'_{12}s'_{11} + c'_{11}s'_{22} + c'_{13}s'_{33} + m_{11}s^* - e'_{31}E'_3, \\ \sigma'_{33} = c'_{13}s'_{11} + c'_{13}s'_{22} + c'_{33}s'_{33} + m_{33}s^* - e'_{33}E'_3, \\ \sigma'_{32} = 2c'_{44}s'_{32} - e'_{15}E'_2, \\ \sigma'_{31} = 2c'_{44}s'_{31} - e'_{15}E'_1, \\ \sigma'_{12} = 2c'_{66}s'_{12}, \\ D'_1 = 2e'_{15}s'_{13} + \varepsilon'_{11}E'_1 + A_{11}E_1^*, \\ D'_2 = 2e'_{15}s'_{23} + \varepsilon'_{11}E'_2 + A_{11}E_2^*, \\ D'_3 = e'_{31}s'_{11} + e'_{31}s'_{22} + e'_{33}s'_{33} + \varsigma_3\varepsilon^* + \varepsilon'_{33}E'_2 + A_{33}E_3^*, \\ D_1^* = A_{11}E'_1 + \varepsilon_{11}^*E_1^*, \\ D_2^* = A_{11}E'_2 + \varepsilon_{11}^*E_2^*, \\ D_3^* = e_3^*\varepsilon^* + A_{33}E'_3 + \varepsilon_{33}^*E_3^*. \end{array} \right. \quad (13)$$

Substituting Eqs. (11), (12), and (13) into Eq. (9) yields

$$c'_{44}\left(\frac{\partial^2 w^p}{\partial x^2} + \frac{\partial^2 w^p}{\partial y^2}\right) + e'_{15}\left(\frac{\partial^2 \varphi^p}{\partial x^2} + \frac{\partial^2 \varphi^p}{\partial y^2}\right) = \rho^p \frac{\partial^2 w^p}{\partial t^2}, \quad (14)$$

$$e'_{15}\left(\frac{\partial^2 w^p}{\partial x^2} + \frac{\partial^2 w^p}{\partial y^2}\right) - \varepsilon_{11}^p\left(\frac{\partial^2 \varphi^p}{\partial x^2} + \frac{\partial^2 \varphi^p}{\partial y^2}\right) = 0, \quad (15)$$

where

$$\rho^p = (\rho_{11})_{33} - (\rho_{12})_{33}^2/(\rho_{22})_{33}, \quad \varepsilon_{11}^p = \varepsilon'_{11} - A_{11}^2/\varepsilon_{11}^*, \quad \nabla^2 \varphi^* = -\frac{A_{11}}{\varepsilon_{11}^*} \nabla^2 \varphi^p. \quad (16)$$

3 Solution of the problem

3.1 Solution for the FGM layer

We assume the solution of the displacement component for the FGM as follows:

$$w^f(x, y, t) = W^f(x)e^{ik(y-ct)}. \quad (17)$$

Substituting Eq. (17) into Eq. (7) yields

$$\frac{d^2 W^f(x)}{dx^2} + \frac{g'}{g} \frac{dW^f(x)}{dx} + k^2 \left(\frac{c^2}{g(\beta_1)^2} - \frac{\sigma_y^0}{gc_{44}^0} - 1 \right) W^f(x) = 0. \quad (18)$$

We introduce the following transformation:

$$W^f(x) = e^{\int \psi(x) dx}. \quad (19)$$

Now, Eq. (18) is converted to the following form:

$$\psi^2 + \frac{g'}{g}\psi + \psi' + k^2 \left(\frac{c^2}{g(\beta_1)^2} - \frac{\sigma_y^0}{gc_{44}^0} - 1 \right) = 0, \quad (20)$$

where g' and ψ' are derivatives of g and ψ w.r.t. x .

To solve Eq. (20), which is a non-linear differential equation in ψ , we expand ψ as follows:

$$\psi = \psi_0 k + \psi_1 + \psi_2 k^{-1} + \psi_3 k^{-2} + \dots \quad (21)$$

Substituting Eq. (21) into Eq. (20) yields

$$\begin{aligned} & \left(\psi_0^2 + \left(\frac{c^2}{g(\beta_1)^2} - \frac{\sigma_y^0}{gc_{44}^0} - 1 \right) \right) k^2 + \left(\psi_0' + 2\psi_0\psi_1 + \frac{g'}{g}\psi_0 \right) k \\ & + \left(\psi_1' + 2\psi_0\psi_2 + \psi_1^2 + \frac{g'}{g}\psi_1 \right) + \left(\psi_2' + 2\psi_0\psi_3 + 2\psi_1\psi_2 + \frac{g'}{g}\psi_2 \right) k^{-1} + \dots = 0. \end{aligned} \quad (22)$$

Then, we get the following equations when the coefficients of each power of k are equated to zero:

$$\begin{cases} \psi_0^2 + \left(\frac{c^2}{g(\beta_1)^2} - \frac{\sigma_y^0}{gc_{44}^0} - 1 \right) = 0, \\ \psi_0' + 2\psi_0\psi_1 + \frac{g'}{g}\psi_0 = 0, \\ \psi_1' + 2\psi_0\psi_2 + \psi_1^2 + \frac{g'}{g}\psi_1 = 0, \\ \psi_2' + 2\psi_0\psi_3 + 2\psi_1\psi_2 + \frac{g'}{g}\psi_2 = 0, \\ \vdots \end{cases} \quad (23)$$

Let $g(x) = e^{\alpha x}$. Then, Eq. (23) gives the solutions of $\psi_0, \psi_1, \psi_2, \dots$ as follows:

$$\begin{cases} \psi_0 = \pm qi, \\ \psi_1 = -\frac{\alpha}{4} \left(1 - \frac{1}{q^2} \right), \\ \psi_2 = \alpha^2 \frac{3q^4 + 6q^2 - 5}{32q^5}, \\ \vdots \end{cases} \quad (24)$$

where

$$q = \sqrt{\left(\frac{c^2}{\beta_1^2} - \frac{\sigma_y^0}{c_{44}^0} \right) e^{-\alpha x} - 1}.$$

Now, we take two solutions (ψ_0, ψ_1) , and substitute them into Eq. (21). Then, using Eq. (19), we get the solution of Eq. (18) as follows:

$$W^f(x) = \frac{1}{\sqrt{q}} e^{-\frac{1}{2}\alpha x} (A_1 e^{i\frac{2k}{\alpha}(\arctan q - q)} + A_2 e^{-i\frac{2k}{\alpha}(\arctan q - q)}), \quad (25)$$

where A_1 and A_2 are unknown constants.

Substituting Eq. (25) into Eq. (17) yields the solution of the mechanical displacement in the FGM layer as follows:

$$w^f(x, y, t) = \frac{1}{\sqrt{q}} e^{-\frac{1}{2}\alpha x} (A_1 e^{i\frac{2k}{\alpha}(\arctan q - q)} + A_2 e^{-i\frac{2k}{\alpha}(\arctan q - q)}) e^{ik(y - ct)}. \quad (26)$$

Solving Eq. (7b), we obtain the electric potential function in the layer as follows:

$$\varphi^f(x, y, t) = (A_3 e^{kx} + A_4 e^{-kx}) e^{ik(y - ct)}. \quad (27)$$

3.2 Solution for the PP substrate

We assume the solution of the mechanical displacement component and the electric potential function for the porous piezoelectric material as follows:

$$w^p(x, y, t) = W^p(x)e^{ik(y-ct)}, \quad (28a)$$

$$\varphi^p(x, y, t) = \varphi^p(x)e^{ik(y-ct)}. \quad (28b)$$

Putting Eqs. (28a) and (28b) into Eqs. (14) and (15), we get

$$c'_{44} \left(\frac{d^2 W^p}{dx^2} - k^2 W^p \right) + e'_{15} \left(\frac{d^2 \varphi^p}{dx^2} - k^2 \varphi^p \right) = -k^2 c^2 \rho^p W^p, \quad (29a)$$

$$e'_{15} \left(\frac{d^2 W^p}{dx^2} - k^2 W^p \right) - \varepsilon_{11}^p \left(\frac{d^2 \varphi^p}{dx^2} - k^2 \varphi^p \right) = 0. \quad (29b)$$

Then, we have

$$W^p(x, y, t) = A_5 e^{-kdx} + B_5 e^{kdx},$$

where

$$d = \sqrt{1 - \frac{c^2}{\beta_2^2}}, \quad \beta_2 = \sqrt{\frac{\bar{c}_{44}}{\rho^p}}, \quad \bar{c}_{44} = c'_{44} + \frac{e'^2_{15}}{\varepsilon_{11}^p}.$$

Here, β_2 represents the bulk shear wave velocity in the PP substrate.

For $x \rightarrow +\infty$, $w^p \rightarrow 0$, and $\varphi^p \rightarrow 0$, the solution of the mechanical displacement and the electric potential function in the porous piezoelectric half-space is obtained as follows:

$$w^p(x, y, t) = A_5 e^{-kdx} e^{ik(y-ct)}, \quad (30)$$

$$\varphi^p(x, y, t) = \left(A_6 e^{-kx} + \frac{e'_{15}}{\varepsilon_{11}^p} A_5 e^{-kdx} \right) e^{ik(y-ct)}. \quad (31)$$

4 Boundary conditions and dispersion relations

(i) When the surface of the FGM layer is electrically open,

$$\sigma_{13} = 0, \quad D_x = 0 \quad \text{at} \quad x = -h_1. \quad (32)$$

(ii) When the surface of the FGM layer is electrically short,

$$\sigma_{13} = 0, \quad \varphi^f = 0 \quad \text{at} \quad x = -h_1. \quad (33)$$

(iii) The continuity conditions at the interface of the FGM layer and the porous piezoelectric substrate, i.e., at $x = 0$, are

$$w^f = w^p, \quad \varphi^f = \varphi^p, \quad \sigma_{13} = \sigma'_{13}, \quad D_x = D'_x + D_x^*. \quad (34)$$

4.1 Dispersion relation for the electrically open case

Using Eqs. (26), (27), (30), and (31) along with the boundary conditions (32) and (34), we obtain the following equations:

$$A_1 Q_1 + A_2 Q_1^* = 0, \quad (35)$$

$$A_3 k \varepsilon e^{-kh_1} - A_4 k \varepsilon e^{kh_1} = 0, \quad (36)$$

$$A_1 \frac{P_0}{\sqrt{q_0}} + A_2 \frac{P_0^*}{\sqrt{q_0}} - A_5 = 0, \quad (37)$$

$$A_3 + A_4 - A_5 \frac{e_{15}}{\varepsilon_{11}^p} - A_6 = 0, \quad (38)$$

$$A_1 \left(-\frac{\mu_0}{4q_0^{5/2}} Q_0 \right) + A_2 \left(-\frac{\mu_0}{4q_0^{5/2}} Q_0^* \right) + A_5 (\bar{c}_{44} k d) + A_6 (k e_{15}) = 0, \quad (39)$$

$$A_3 k \varepsilon - A_4 k \varepsilon + A_5 \left(-k d e_{15} \left(\frac{t_{11}}{\varepsilon_{11}^p} + \frac{t_{12}}{\varepsilon_{11}^p} - 1 \right) \right) + A_6 (-k(t_{11} + t_{12})) = 0, \quad (40)$$

where

$$\left\{ \begin{array}{l} P_0 = e^{i \frac{2k}{\alpha} (\arctan q_0 - q_0)}, \quad P_0^* = e^{-i \frac{2k}{\alpha} (\arctan q_0 - q_0)}, \\ P_1 = e^{i \frac{2k}{\alpha} (\arctan q_1 - q_1)}, \quad P_1^* = e^{-i \frac{2k}{\alpha} (\arctan q_1 - q_1)}, \\ q_0 = \sqrt{\frac{c^2}{\beta_1^2} - \frac{\sigma_y^0}{c_{44}^0}} - 1, \quad q_1 = \sqrt{\left(\frac{c^2}{\beta_1^2} - \frac{\sigma_y^0}{c_{44}^0} \right) e^{\alpha h_1}} - 1, \\ Q_0 = P_0 \left(-2(-2iq_0 k + \alpha) + \left(\frac{c^2}{\beta_1^2} - \frac{\sigma_y^0}{c_{44}^0} \right) (-4iq_0 k + \alpha) \right), \\ Q_0^* = P_0^* \left(-2(2iq_0 k + \alpha) + \left(\frac{c^2}{\beta_1^2} - \frac{\sigma_y^0}{c_{44}^0} \right) (4iq_0 k + \alpha) \right), \\ Q_1 = P_1 \left(-2e^{-\alpha h_1} (-2iq_1 k + \alpha) + \left(\frac{c^2}{\beta_1^2} - \frac{\sigma_y^0}{c_{44}^0} \right) (-4iq_1 k + \alpha) \right), \\ Q_1^* = P_1^* \left(-2e^{-\alpha h_1} (2iq_1 k + \alpha) + \left(\frac{c^2}{\beta_1^2} - \frac{\sigma_y^0}{c_{44}^0} \right) (4iq_1 k + \alpha) \right), \\ t_{11} = \varepsilon'_{11} - \frac{A_{11}^2}{\varepsilon_{11}^*} c_v, \quad t_{12} = A_{11}(1 - c_v), \quad c_v = \frac{c_{\varphi^*}^2}{c_{\varphi}^2}, \quad \varepsilon_{11}^p = \varepsilon'_{11} - \frac{A_{11}^2}{\varepsilon_{11}^*}. \end{array} \right.$$

It can be seen that Eqs. (35)–(40) are 6 equations with 6 variables. For non-trivial solutions, the determinant of the coefficient matrix vanishes, which leads to the dispersion relation as follows:

$$|B_{ij}| = 0, \quad i, j = 1, 2, \dots, 6. \quad (41)$$

The non-zero coefficients of the above determinant equation (41) are provided in Appendix A.

4.2 Dispersion relation for the electrically short case

Using Eqs. (26), (27), (30), and (31) along with the boundary conditions (33) and (34), we obtain the equations the same as the above except Eq. (36), which changes as

$$A_3 e^{-kh_1} + A_4 e^{kh_1} = 0. \quad (42)$$

The dispersion relation for the electrically short case is obtained in the determinant form as follows:

$$|B_{ij}^s| = 0, \quad i, j = 1, 2, \dots, 6. \quad (43)$$

The non-zero coefficients of the above determinant equation (43) are provided in Appendix B.

5 Validation of the problem

Case I When the piezoelectric effect is neglected in the lower medium, the considered model reduces into the FGM layer embedded over the elastic substrate. The dispersion relation for the reduced model is obtained as follows:

$$\frac{c'_{44} dk (P_0^* Q_1 - P_0 Q_1^*)}{\sqrt{q_0}} + \frac{c_{44}^0 (-Q_1 Q_0^* + Q_0 Q_1^*)}{4(q_0)^{\frac{5}{2}}} = 0, \quad (44)$$

which resembles with the phase velocity equation of the Love-type wave propagation attained by Qian et al.^[10].

Case II When the considered structure is reduced into a homogeneous isotropic layer lying over a homogeneous isotropic semi-infinite medium, the dispersion relation becomes

$$\tan \left(kh_1 \sqrt{c^2 / \beta_1'^2 - 1} \right) = \frac{c'_{44} \sqrt{1 - c^2 / \beta_2'^2}}{c_{44}^0 \sqrt{c^2 / \beta_1'^2 - 1}}, \quad (45)$$

where

$$\beta_1' = \sqrt{c_{44}^0 / \rho^f}, \quad \beta_2' = \sqrt{c'_{44} / \rho^p}.$$

Equation (45) matches with the classical Love-type wave equation with the condition $\beta_1' < c < \beta_2'$, which is the required sequence of the Love-type wave velocity in the layered structure^[29].

6 Numerical example and result discussion

The data taken for the numerical purpose are given in Table 1.

Table 1 Material properties^[7,25]

Material type	Elastic constant (c_{44})/(10 ¹⁰ N·m ⁻²)	Piezoelectric constant (e_{15})/(C·m ⁻²)	Dielectric constant (10 ⁻¹⁰ F·m ⁻²)	Mass density (ρ)/(kg·m ⁻³)
FGM	$3.05 \times e^{\alpha x}$	—	0.45	7.50×10^3
PZT-5H	2.3	17	$\epsilon'_{11} = 277$ $\epsilon''_{11} = 299$ $A_{11} = 112$	$(\rho_{11})_{33} = 4.950 \times 10^3$ $(\rho_{12})_{33} = -1.125 \times 10^3$ $(\rho_{22})_{33} = 4.800 \times 10^3$

An analytical solution is obtained for the transference of Love-type waves in a composite structure consisting of an FGM layer and a PP substrate. The phase velocity of the considered wave satisfies the condition $\beta_1 < c < \beta_2$, where β_1 and β_2 are the bulk wave velocities in the FGM layer and the PP substrate, respectively. The above condition can also be verified through graphs drawn for the dimensionless phase velocity (c/β_1) versus the dimensionless wave number (kh_1). The range of the dimensionless phase velocity agree well with the condition $\beta_1 < c < \beta_2$.

Using the dispersion relations (41) and (43), numerical examples are given. For the numerical computation, PZT-5H is taken as the porous-piezoelectric layer. The phase velocity of the Love-type wave decreases with the wave number.

Figures 2 and 3 give the variations of the dimensionless phase velocity of the Love-type wave with the dimensionless wave number for different values of the gradient factor of the FGM layer for electrically open and short cases, respectively. We notice that, in both cases, the phase velocity gets reduced with the increase in the gradient factor.

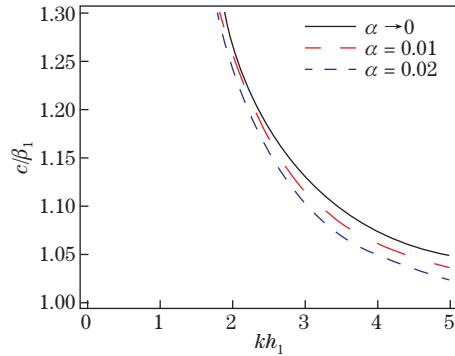


Fig. 2 Dimensionless phase velocity (c/β_1) versus the dimensionless wave number (kh_1) curves for different values of the gradient factor of the FGM layer (α) for the electrically open case

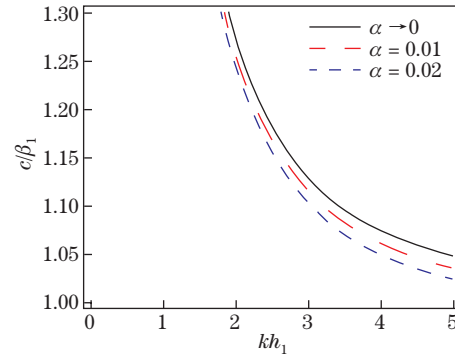


Fig. 3 Dimensionless phase velocity (c/β_1) versus the dimensionless wave number (kh_1) curves for different values of the gradient factor of the FGM layer (α) for the electrically short case

Figures 4 and 5 give the variations of the non-dimensional phase velocity of the Love-type waves with the non-dimensional wave number width of the FGM layer for electrically open and short cases, respectively. It is clearly visible that the phase velocity decreases when the width of the FGM layer increases.

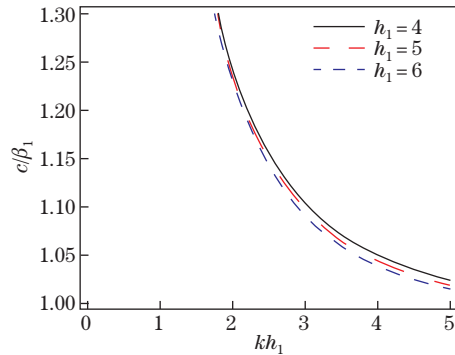


Fig. 4 Dimensionless phase velocity (c/β_1) versus the dimensionless wave number (kh_1) curves for different values of the height of the FGM layer (h_1) for the electrically open case

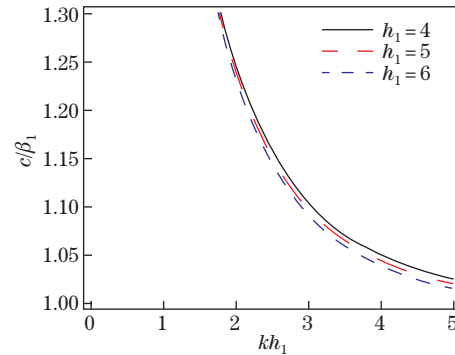


Fig. 5 Dimensionless phase velocity (c/β_1) versus the dimensionless wave number (kh_1) curves for different values of the height of the FGM layer (h_1) for the electrically short case

The effects of the initial stresses on the phase velocity of the Love-type wave in the FGM layer is shown in Figs. 6 and 7 for the tensile stress and the compressive stress, respectively, for the open case.

The effects of the initial stress on the phase velocity of the Love-type wave are shown in Figs. 8 and 9 for the tensile stress and the compressive stress, respectively, for the short case.

It is seen that the initial stress has slight effect on the phase velocity of the Love-type wave. It is noticed that the effect of the initial stress is negligible when $\mu_0 < 10^8$ Pa. When $\mu_0 > 10^8$ Pa, the phase velocity increases with the increase in the tensile stress whereas decreases with the increase in the absolute value of the initial compressive stress.

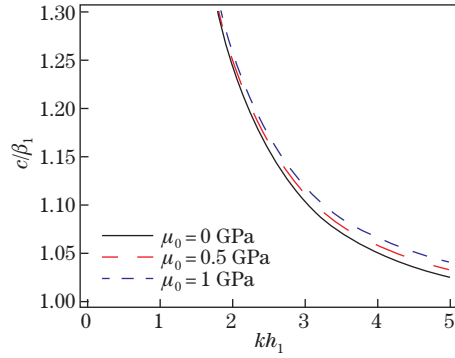


Fig. 6 Dimensionless phase velocity (c/β_1) versus the dimensionless wave number (kh_1) curves for different values of the initial tensile stress (μ_0) for the electrically open case

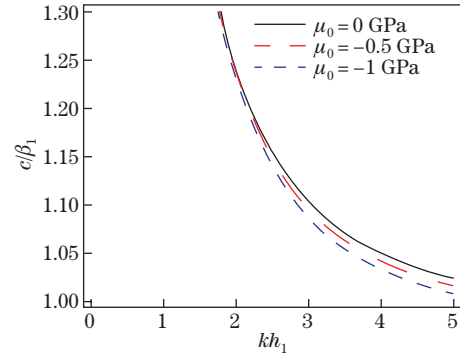


Fig. 7 Dimensionless phase velocity (c/β_1) versus the dimensionless wave number (kh_1) curves for different values of the initial compressive stress (μ_0) for the electrically open case

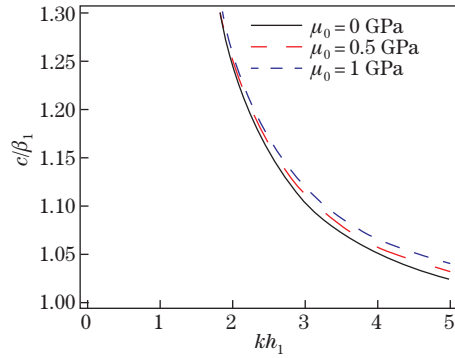


Fig. 8 Dimensionless phase velocity (c/β_1) versus the dimensionless wave number (kh_1) curves for different values of the initial tensile stress (μ_0) for the electrically short case

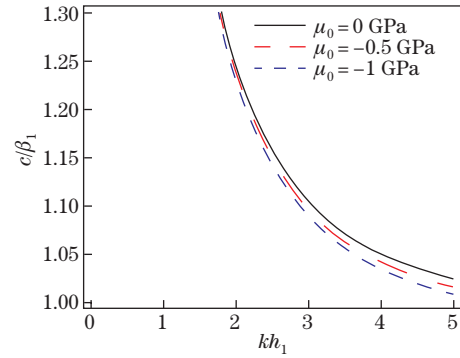


Fig. 9 Dimensionless phase velocity (c/β_1) versus the dimensionless wave number (kh_1) curves for different values of the initial compressive stress (μ_0) for the electrically short case

7 Conclusions

The propagation of Love-type waves in a bedded structure comprising of an FGM layer with a constant initial stress lying over a porous-piezoelectric substrate is taken into consideration. The WKB approximation technique and the variable separable method are applied to obtain the expressions for the mechanical displacement and the electric potential function of the FGM layer and the PP substrate, respectively. Dispersion relations are obtained with the consideration of the appropriate boundary conditions for two cases, i.e., electrically open and electrically short. For the numerical illustrations, the material constants of PZT-5H are taken for the porous-piezoelectric layer. We summarize with the following prominent observations:

- (i) The material gradient of the FGM layer has a significant effect on the phase velocity of Love-type waves. The phase velocity of the considered wave decreases when the gradient factor of the FGM layer increases in both electrically open and short cases.
- (ii) The phase velocity of Love-type waves decreases with the increase in the width of the FGM layer in both electrically open and short cases.
- (iii) The effect of the initial stress is negligible when $|\mu_0| < 10^8$ Pa. The phase velocity of the Love-type wave increases with the increase in the initial tensile stress whereas decreases with

the increase in the absolute magnitude of the initial compressive stress when $|\mu_0| > 10^8$ Pa.

(iv) The present study contributes towards the design and optimization of underwater acoustic devices.

References

- [1] HASHIMOTO, K. *Surface Acoustic Wave Devices in Telecommunications*, Springer-Verlag, Berlin, Heidelberg (2000)
- [2] JONES, R. M. *Mechanics of Composite Materials*, Scripta Book Co., Washington, D. C. (1975)
- [3] SURESH, S. and MORTENSEN, A. *Fundamentals of Functionally Graded Materials*, IOC Communications Ltd., London (1998)
- [4] JHA, D. K., KANT, T., and SINGH, R. K. A critical review of recent research on functionally graded plates. *Composite Structures*, **96**, 833–849 (2013)
- [5] HAN, X., LIU, G. R., LAM, K. Y., and OHYOSHI, T. Quadratic layer element for analyzing stress waves in FGMS and its application in material characterization. *Journal of Sound and Vibration*, **236**, 307–321 (2000)
- [6] HAN, X. and LIU, G. R. Effects of SH waves in a functionally graded plate. *Mechanics Research Communication*, **29**, 327–338 (2002)
- [7] QIAN, Z., JIN, F., WANG, Z., and KISHIMOTO, K. Transverse surface waves on a piezoelectric material carrying a functionally graded layer of finite thickness. *International Journal of Engineering Science*, **45**, 455–466 (2007)
- [8] ZHANG, G. M. and BATRA, R. C. Wave propagation in functionally graded materials by modified smoothed particle hydrodynamics (MSPH) method. *Journal of Computational Physics*, **222**, 374–390 (2007)
- [9] BIN, W., JIANGONG, Y., and CUNFU, H. Wave propagation in non-homogeneous magneto-electro-elastic plates. *Journal of Sound and Vibration*, **317**, 250–264 (2008)
- [10] QIAN, Z. H., JIN, F., KISHIMOTO, K., and LU, T. Propagation behavior of Love waves in a functionally graded half-space with initial stress. *International Journal of Solids and Structures*, **46**, 1354–1361 (2009)
- [11] AKSOY, H. G. and ŞNOCAK, E. Wave propagation in functionally graded and layered materials. *Finite Elements in Analysis and Design*, **45**, 876–891 (2009)
- [12] RAVASOO, A. Counter-propagation of harmonic waves in exponentially graded materials. *Journal of Sound and Vibration*, **330**, 3874–3882 (2011)
- [13] CAO, X., JIN, F., and JEON, I. Calculation of propagation properties of Lamb waves in a functionally graded material (FGM) plate by power series technique. *NDT and E International*, **44**, 84–92 (2011)
- [14] KIELCZYŃKI, P., SZALEWSKI, M., BALCERZAK, A., and WIEJA, K. Propagation of ultrasonic Love waves in nonhomogeneous elastic functionally graded materials. *Ultrasonics*, **65**, 220–227 (2016)
- [15] ARANI, A. G., KOLAHCHI, R., and BARZOKI, A. M. Effect of material in-homogeneity on electro-thermo-mechanical behaviors of functionally graded piezoelectric rotating shaft. *Applied Mathematical Modelling*, **35**, 2771–2789 (2011)
- [16] SAHU, S. A., MONDAL, S., and DEWANGAN, N. Polarized shear waves in functionally graded piezoelectric material layer sandwiched between corrugated piezomagnetic layer and elastic substrate. *Journal of Sandwich Structures and Materials* (2017) <https://doi.org/10.99636217726330>
- [17] SINGHAL, A., SAHU, S. A., and CHAUDHARY, S. Approximation of surface wave frequency in piezo-composite structure. *Composites Part B: Engineering*, **144**, 19–28 (2018)
- [18] MONDAL, S. and SAHU, S. A. Propagation of SH waves in corrugated FGPM layer lying over a piezomagnetic half-space. *Mechanics of Advanced Materials and Structures*, **26**, 39–34 (2019)
- [19] CRACIUN, F., GUIDARELLI, G., GALASSI, C., and RONCARI, E. Elastic wave propagation in porous piezoelectric ceramics. *Ultrasonics*, **36**, 427–430 (1998)

- [20] ZENG, T., DONG, X. L., MAO, C. L., ZHOU, Z. Y., and YANG, H. Effects of pore shape and porosity on the properties of porous PZT 95/5 ceramics. *Journal of the European Ceramic Society*, **27**, 2025–2029 (2007)
- [21] WANG, Q., CHEN, Q., ZHU, J., HUANG, C., DARVELL, B. W., and CHEN, Z. Effects of pore shape and porosity on the properties of porous LKN ceramics as bone substitute. *Materials Chemistry and Physics*, **109**, 488–491 (2008)
- [22] PIAZZA, D., CAPIANI, C., and GALASSI, C. Piezoceramic material with anisotropic graded porosity. *Journal of the European Ceramic Society*, **25**, 3075–3078 (2005)
- [23] KAR-GUPTA, R. and VENKATESH, T. A. Electromechanical response of porous piezoelectric materials. *Acta Materialia*, **54**, 4063–4078 (2006)
- [24] VASHISHTH, A. K. and GUPTA, V. Vibrations of porous piezoelectric ceramic plates. *Journal of Sound and Vibration*, **325**, 781–797 (2009)
- [25] VASHISHTH, A. K., DAHIYA, A., and GUPTA, V. Generalized Bleustein-Gulyaev type waves in layered porous piezoceramic structure. *Applied Mathematics and Mechanics (English Edition)*, **36**(9), 1223–1242 (2015) <https://doi.org/10.1007/s10483-015-1976-6>
- [26] GAUR, A. M. and RANA, D. S. Dispersion relations for SH waves propagation in a porous piezoelectric (PZT-PVDF) composite structure. *Acta Mechanica*, **226**, 4017–4029 (2015)
- [27] VASHISHTH, A. K. and GUPTA, V. 3-D waves in porous piezoelectric materials. *Mechanics of Materials*, **80**, 96–112 (2015)
- [28] BAROI, J., SAHU, S. A., and SINGH, M. K. Dispersion of polarized shear waves in viscous liquid over a porous piezoelectric substrate. *Journal of Intelligent Material System and Structures*, **29**, 2040–2048 (2018)
- [29] EWING, W. M., JARDETZKY, W. S., PRESS, F., and BEISER, A. *Elastic Waves in Layered Media*, McGraw-Hill, New York (1957)

Appendix A

$$\begin{aligned}
 B_{11} &= Q_1, & B_{12} &= Q_1^*, \\
 B_{23} &= k\varepsilon e^{-kh_1}, & B_{24} &= -k\varepsilon e^{kh_1}, \\
 B_{31} &= \frac{P_0}{\sqrt{q_0}}, & B_{32} &= \frac{P_0^*}{\sqrt{q_0}}, & B_{35} &= -1, \\
 B_{43} &= 1, & B_{44} &= 1, & B_{45} &= -\frac{e_{15}}{\varepsilon_{11}^p}, & B_{46} &= -1, \\
 B_{51} &= -\frac{\mu_0}{4q_0^{5/2}}Q_0, & B_{52} &= -\frac{\mu_0}{4q_0^{5/2}}Q_0^*, & B_{55} &= \bar{c}_{44}kd, & B_{56} &= ke_{15}, \\
 B_{63} &= k\varepsilon, & B_{64} &= -k\varepsilon, & B_{65} &= -kde_{15}\left(\frac{t_{11}}{\varepsilon_{11}^p} + \frac{t_{12}}{\varepsilon_{11}^p} - 1\right), & B_{66} &= -k(t_{11} + t_{12}).
 \end{aligned}$$

Appendix B

$$\begin{aligned}
 B_{11}^s &= Q_1, & B_{12}^s &= Q_1^*, \\
 B_{23}^s &= e^{-kh_1}, & B_{24}^s &= e^{kh_1}, \\
 B_{31}^s &= \frac{P_0}{\sqrt{q_0}}, & B_{32}^s &= \frac{P_0^*}{\sqrt{q_0}}, & B_{35}^s &= -1, \\
 B_{43}^s &= 1, & B_{44}^s &= 1, & B_{45}^s &= -\frac{e_{15}}{\varepsilon_{11}^p}, & B_{46}^s &= -1, \\
 B_{51}^s &= -\frac{\mu_0}{4q_0^{5/2}}Q_0, & B_{52}^s &= -\frac{\mu_0}{4q_0^{5/2}}Q_0^*, & B_{55}^s &= \bar{c}_{44}kd, & B_{56}^s &= ke_{15}, \\
 B_{63}^s &= k\varepsilon, & B_{64}^s &= -k\varepsilon, & B_{65}^s &= -kde_{15}\left(\frac{t_{11}}{\varepsilon_{11}^p} + \frac{t_{12}}{\varepsilon_{11}^p} - 1\right), & B_{66}^s &= -k(t_{11} + t_{12}).
 \end{aligned}$$